ACS Macro Letters

Letter

pubs.acs.org/macroletters

Post-Electrospinning "Triclick" Functionalization of Degradable Polymer Nanofibers

Jukuan Zheng,[†] Geng Hua,[†] Jiayi Yu,[†] Fei Lin,[†] Mary Beth Wade,[§,†] Darrell H. Reneker,[†] and Matthew L. Becker*[,†,‡]

[†]Department of Polymer Science, [‡]Department of Biomedical Engineering, and [§]Integrated Bioscience Program, The University of Akron, Akron, Ohio 44325, United States

Supporting Information

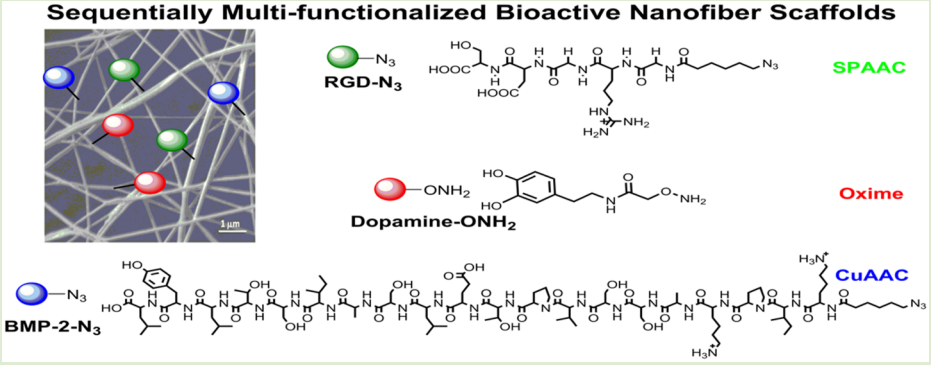

ABSTRACT: 4-Dibenzocyclooctynol (DIBO) was used as an initiator for the ring-opening copolymerization of ε-caprolactone and 1,4,8-trioxaspiro[4.6]-9-undecanone (TOSUO) resulting in a series of DIBO end-functionalized copolymers. Following deprotection of the ketone group, the polymers were derivatized with aminooxyl-containing compounds by oxime ligation. Mixtures of keto- and alkyne-derivatized polymers were co-electrospun into well-defined nanofibers containing three separate chemical handles. Strain-promoted azide alkyne cycloaddition (SPAAC), oxime ligation, and copper-catalyzed azide alkyne cycloaddition (CuAAC) were used to sequentially functionalize the nanofibers first with fluorescent reporters and then separately with bioactive Gly-Arg-Gly-Asp-Ser (GRGDS), BMP-2 peptide, and dopamine. This translationally relevant approach facilitates the straightforward derivatization of diverse bioactive molecules that can be controllably tethered to the surface of nanofibers.

Polymeric nanofibers have been studied extensively for applications in wound healing and regenerative medicine.[1] Most polymers can be fabricated into nanofibers via melt or electrospinning with highly tunable size and morphology by manipulating various experimental parameters.[2] Nanofibers have been found to influence cell function in a number of ways including morphology, confinement via contact guidance, and mechanical properties.[3,4] While there have been several reports of methods for placing bioactive groups on nanofibers,[5−8] degradable polymers present some significant limitations with regard to conjugation chemistry. To preserve the structural and morphological integrity of the nanofibers, any conjugation method must be compatible with a solvent system orthogonal to the solubility parameters of the polymer. One strategy to overcome this limitation has been to introduce the bioactive species prior to electrospinning.[9,10] While some have successfully utilized this approach, it is inefficient in that a significant fraction of the bioactive species are buried in the nanofiber and, as such, are not bioavailable to the target cell population. The lack of control over surface functionality severely complicates any manufacturing process and regulatory strategy when trying to advance these materials to clinical applications.

There have been several demonstrations of peptide-modified nanofibers in biomedicine including bone,[11] neural,[12−14] and vascular applications.[15,16] However, other than integrin-mediated adhesion via Gly-Arg-Gly-Asp-Ser (GRGDS) peptides, there are no reports describing the use and utility of multiple (≥3) bioactive groups attached to nanofibers. However, in higher organisms, it is well established that multiple bioactive molecules work synergistically in time- and concentration-dependent manners to regulate any number of cellular functions.[17−19] In order to mimic these complex interactions, strategies for controllably derivatizing electrospun nanofibers are needed to advance our understanding of cellular behavior *in vitro* and *in vivo*. It would therefore be invaluable to create a platform scaffold that could be derivatized post-fabrication with multiple bioactive species using highly controlled techniques.

Received: December 2, 2014
Accepted: January 21, 2015
Published: January 26, 2015

DOI: 10.1021/mz500759n
ACS Macro Lett. 2015, 4, 207−213

A number of chemical methods have been used to decorate nanofibers with peptides and carbohydrates. However, conjugating bioactive groups on degradable nanofibers is challenging. Currently, there are a few examples showing chemical modification of nanofibers without plasma or hydrolytic methods.[6] Several "click" methods[20] including thiol−ene,[21] copper-catalyzed azide alkyne cycloaddition (CuAAC),[21,22] Diels−Alder addition,[23,24] and aminolysis[25] have been utilized for the surface modification of nanofibers. Strain-promoted azide alkyne cycloaddition (SPAAC) is another method for functionalizing nanofibers due to its efficient and bio-orthogonal characteristics.[26] SPAAC has been used extensively for bioimaging,[27−31] hydrogel fabrication,[32−35] nanofiber,[18,36,37] surface,[38−41] and polymer functionalization.[42] Oxime ligation methods are also gaining popularity for polymer,[38,43] protein,[44] surface,[45,46] and hydrogel modification.[47,48]

In our research, CuAAC, SPAAC, and oxime ligation are used in combination for the first time to generate trifunctionalized nanofiber scaffolds. We aim to use these highly functional materials to explore the synergistic and concentration-dependent influence of combinations of bioactive molecules on cellular systems. Herein, we report the synthesis and characterization of sequential "triclick" modification methods of nanofiber-based scaffolds, first with fluorescent reporters and then separately using bioactive molecules. To the best of our knowledge, functionalizing degradable nanofibers with multiple biomolecules has not been reported previously.

4-Dibenzocyclooctynol (DIBO) was used as the initiator for the ring-opening copolymerization of ε-caprolactone (ε-CL) and 1,4,8-trioxaspiro[4.6]-9-undecanone (TOSUO)[49] to yield the functional copolymer DIBO-(P(CL-*co*-OPD)). As shown in Figure 1, polymers with similar molecular mass possessing different molar concentrations of TOSUO repeat units were obtained. Post-polymerization deprotection of the cyclic acetal groups proceeded under mild conditions resulting in the recovery of the reactive ketone group, which was confirmed by ^{1}H NMR spectroscopy (Figure 2B). Successful polymerizations were demonstrated by ^{1}H NMR (Figure 2A) and size exclusion chromatography (SEC) (Figure 1). As shown in Figure 2A, DIBO-end-functionalized polymers were successfully obtained. The proton resonances from DIBO are visible within the inset images (Supporting Information (SI)), indicating that the strained alkyne in the DIBO molecule survived the polymerization conditions. Using a number of different feed ratios, polymers possessing variable concentrations of the TOSUO monomer were obtained. The extent of TOSUO incorporation trends with the feed ratio while maintaining relatively narrow molecular mass distributions (Figure 1). As shown in Figure 2B, resonances at δ = 3.90 and 4.10 ppm, corresponding to protons on the cyclic acetal protecting $-CH_2CH_2-$ group, disappeared, and new peaks (δ = 2.50 and 2.60 ppm) corresponding to the resonances from the adjacent methylene (CH_2) emerged.

Further modification of the ketone group was carried out using *O*-(prop-2-yn-1-yl)hydroxylamine hydrochloride or *O*-(pent-4-en-1-yl)hydroxylamine hydrochloride. Figure 2C and 2D shows resonances corresponding to the oxime condensation peaks of each of the two different hydroxylamine compounds. The preservation of DIBO functionality following the deprotection step and the extent of functionalization was confirmed by UV−visible spectroscopy (SI). The conversion

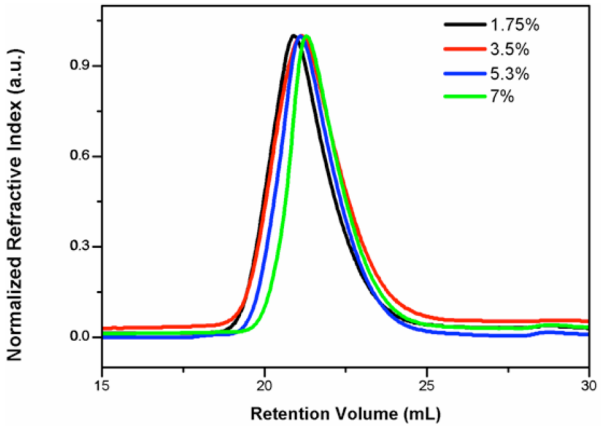

Feed Ratio	1.75%	3.50%	5.30%	7%
Composition	3.15%	4.70%	5.55%	7%
Mn/10^3	20.9	20.6	20.4	17.6
$Đ_m$	1.16	1.23	1.19	1.16

Figure 1. SEC traces of resulting polymers obtained from DIBO-initiated ring-opening polymerization (ROP) of ε-CL and TOSUO. Different feed ratios of the TOSUO monomer resulted in polymers possessing similar molecular mass and mass distribution but different molar ratios of ketone containing monomer repeat units. The incorporation of ketone-containing repeat units was measured using ^{1}H NMR spectroscopy.

steps yielded polymer 1 and polymer 2 (Scheme 1). A 40% solution of a 1:1 mixture (mass) of polymer 1 and polymer 2 (5.5% ketone) in DMF/DCM (1/4 v/v) was electrospun to generate nanofiber mats possessing DIBO, ketone, and alkyne groups on the surface that are available for post-fabrication functionalization via SPAAC, oxime, and CuAAC reactions using conditions that do not degrade the nanofiber mats.

Optimized electrospinning conditions yielded nanofibers with diameters measuring approximately 300 nm (SEM imaging, SI). The nanofiber mats were then derivatized with three different fluorescent molecules to demonstrate the presence and availability of the individual reactive groups on the surface of the nanofiber and that the reaction conditions did not lead to nanofiber degradation.

As observed in Figure 3A, green fluorescence indicates that the SPAAC reaction between the DIBO and Chromeo 488 azide occurred successfully, while the control experiment showed no fluorescence due to nonspecific adsorption in accordance with previous results.[37] Any residual DIBO groups were then consumed using a secondary CH_3O-PEG_{1k}-N_3 (2 mg/mL) incubation. For the oxime reaction, Chromeo 488 azide-treated nanofibers were incubated with Alexa Fluor 568 hydrazide for 5 min. Following the wash procedure, images showing red fluorescence (Figure 3B) were captured with no change in image acquisition settings aside from switching the filter cube. The control experiment (PCL fibers) showed no fluorescence under identical imaging conditions. Similarly, the third image in Figure 3C was taken using a DAPI filter cube, where the presence of blue fluorescence provides evidence of the conjugation of 9-methyleneazidoanthracene. As the control experiment did not exhibit any fluorescence, it was determined

DOI: 10.1021/mz500759n
ACS Macro Lett. 2015, 4, 207−213

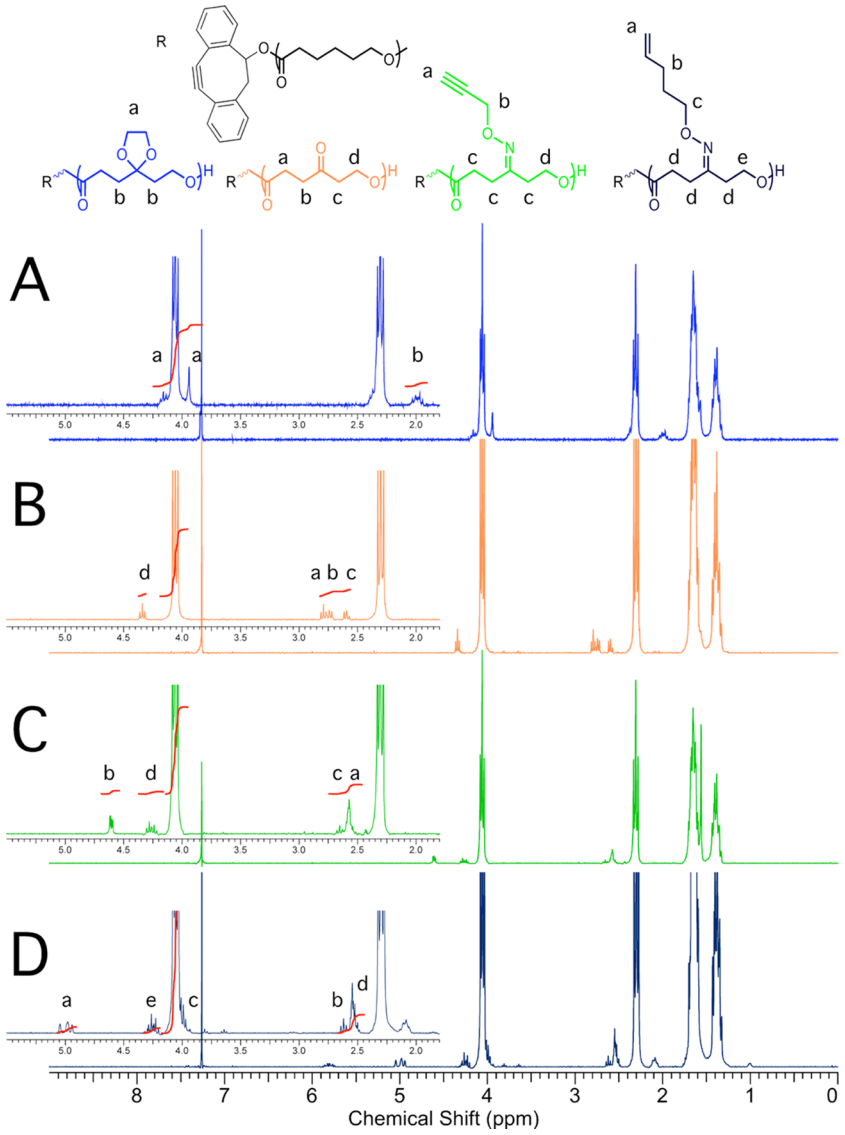

Figure 2. ^{1}H NMR spectra of DIBO-(P(CL-*co*-OPD)) polymers. Individually these spectra show the successful polymerization (A), deprotection of the cyclic acetal (B), and oxime ligation with *O*-(prop-2-yn-1-yl)hydroxylamine hydrochloride (C) and *O*-(pent-4-en-1-yl)hydroxylamine hydrochloride (D).

Scheme 1. Synthetic Route for Desired Polymers with DIBO, Ketone, Alkyne, and Alkene Functional Groups[a]

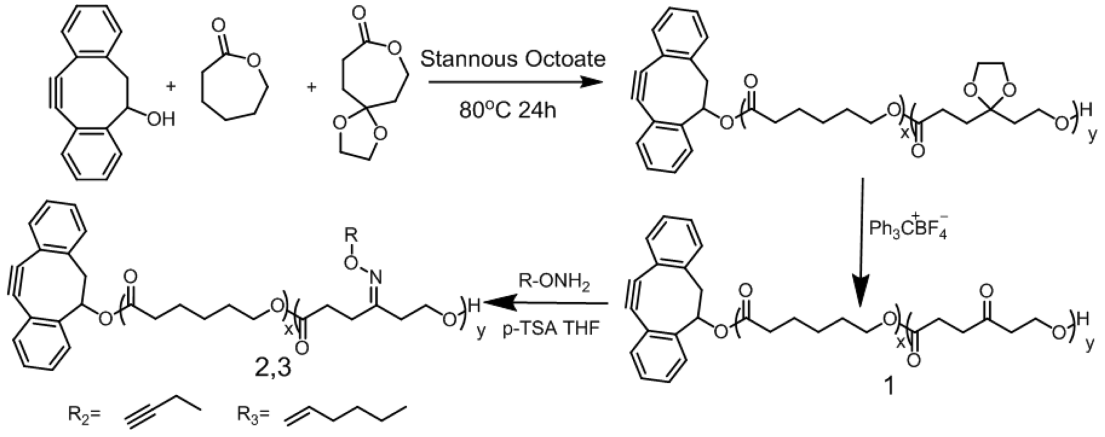

[a]Control over the molar extent of ketone functionality and diversity in the available oxime functional species enables a wide variety of potential functional group combinations.

DOI: 10.1021/mz500759n
ACS Macro Lett. 2015, 4, 207−213

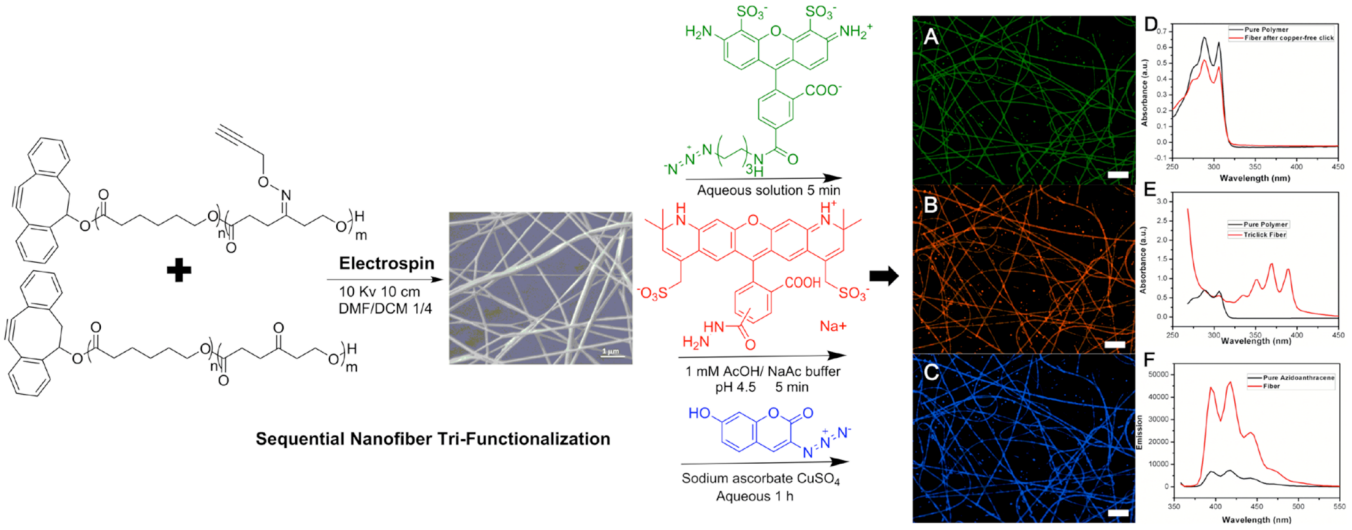

Figure 3. (A–C) Fluorescence images showing successful sequential trifunctionalization of fibers. The scale bar is 20 μm for all images (D–F). UV–visible absorption spectra show evidence of the successful copper-free click reaction and copper-catalyzed reaction by the reduced DIBO signal and the appearance of the 9-methyleneazidoanthracene signal at 306 nm and 325–400 nm, respectively.

that the capping of DIBO groups with oligoethylene glycol was successful, and the resultant fluorescence was due to CuAAC conjugation rather than additional SPAAC reaction.

Fluorescence microscopy was used to visualize the modifications. Control experiments performed using nanofibers without DIBO and ketone groups for the SPAAC and oxime reaction, respectively, resulted in no fluorescence. For the CuAAC reaction, the control experiment was done using the CH_3O-PEG-N_3 capped DIBO-PCL nanofiber. The UV–visible spectra showed a decrease in the absorbance of DIBO (306 nm) due to SPAAC reaction as shown in Figure 3D.[37] Following the oxime reaction, there is no significant change in the UV–visible spectra, as alkene groups do not possess strong absorbance characteristics. After the CuAAC reaction with 9-methyleneazidoanthracene, the absorbance transition in the range of 325–400 nm in Figure 3E arises from 9-methyleneazidoanthracene. An observable absorbance at 306 nm is also present, which corresponds to DIBO groups that are buried inside the nanofibers. 9-Methyleneazidoanthracene was shown to have the expected click-induced fluorescence enhancement, and the fluorescence emission spectra was measured to show that chemical conjugation, rather than physical adsorption, occurred on the nanofibers. The triclicked nanofiber solution was diluted, and its absorbance and emission spectra were compared with a standardized solution of pure 9-methyleneazidoanthracene. A similar absorbance (SI) in the range of 325–400 nm for both the nanofiber solution and the pure anthracene solution standard indicates that these two solutions have a comparable concentration of anthracene. As shown in Figure 3F, the nanofiber solution exhibited greater fluorescence emission than the control proving there was a click-induced fluorescence enhancement.

To further demonstrate three successful sequential modifications by separate methods, ^{1}H NMR spectra of the modified nanofibers are provided. In Figure 4A, the peak at δ 3.65 ppm shows the modification by SPAAC. Figure 4B also shows the expected proton resonances of molecule 3 at about δ = 5.0 and 2.1 ppm. Finally, the appearance of resonances at δ = 6.6, 8.1, 8.35, and 8.6 ppm verify the modification of nanofibers via CuAAC. The percentage of functionalization using these three reactions was calculated to be 27.0 ± 3.5%, 17.4 ± 3.8%, and 36.2 ± 5.5%, respectively, by comparing the integration values of the PEG chain (δ = 3.65 ppm), aminooxyl-containing molecule (δ = 5.0 ppm), and 9-methyleneazidoanthracene (δ = 6.56 ppm) to that of the PCL backbone (δ = 4.09 ppm) from the ^{1}H NMR spectra. Three repeats were carried out at the same time for each step modification (SI).

While the fluorescent probes demonstrated the ability to derivatize the nanofibers with three separate functional groups, our translational goals seek to use nanofibers with multiple bioactive molecules to direct cell response. To show that we are able to fabricate bioactive nanofiber-based scaffolds using this sequential triclick method, the adhesive peptide sequence GRGDS, a tethered calcium-binding dopamine species, and an osteoinductive BMP-2 peptide sequence were chosen as models to demonstrate the reliability of this methodology for multiple bioactive motif conjugations. Tethering multiple bioactive molecules to a scaffold in a highly efficient and well-defined manner is required for translational relevance. As long as the solvent used to dissolve the bioactive group does not dissolve the nanofiber, there is no limit to the type of diversity of molecule that can be attached as long as the complementary functional group is present on the molecule in such a way that it is not hindered sterically.

N_3-GRGDS, NH_2O-dopamine, and N_3-BMP-2 peptide were attached to the nanofibers sequentially via SPAAC, oxime, and CuAAC, similar to the methods described above. RGD was chosen due to its widely understood role in the promotion of cell adhesion.[50−52] Dopamine was chosen due to its binding affinity with calcium ions, which have previously been shown to promote the development of hydroxyapatite in simulated body fluid (SBF).[53] BMP-2 peptide was chosen for its significant osteoinductive effects *in vitro* and *in vivo*.[54,55] We have also demonstrated recently that combinations of tethered BMP-2 and GRGDS sequences are able to synergistically increase the proliferative potential and accelerate the differentiation timeline of human mesenchymal stem cells.[56] The combination of these three bioactive molecules on the surface of nanofibers enables the investigation of concentration-dependent synergistic effects on directed osteogenesis and bone healing processes.

DOI: 10.1021/mz500759n
ACS Macro Lett. 2015, 4, 207–213

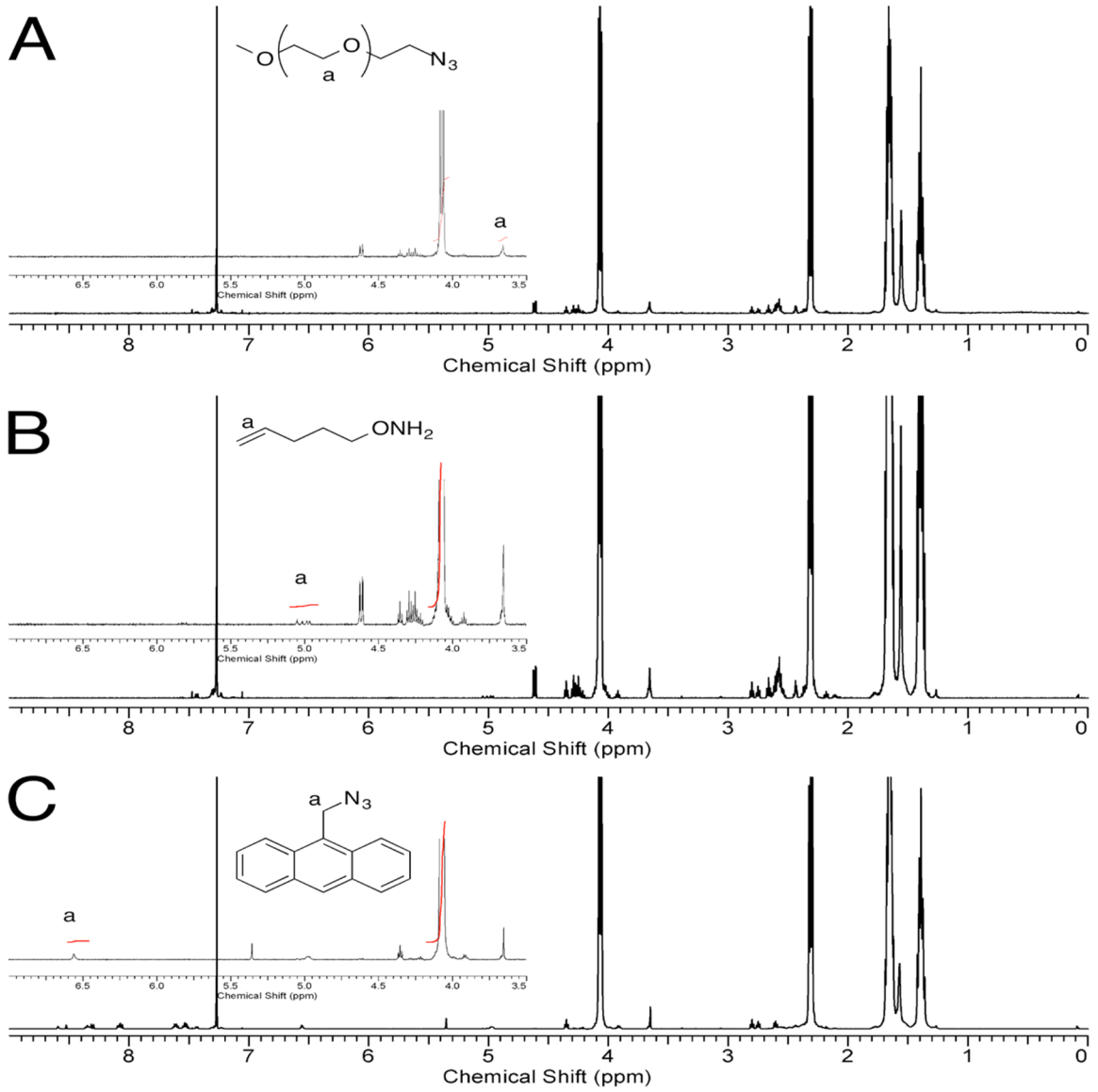

Figure 4. ^{1}H NMR spectra show the successful sequential "triclick" modification of the nanofibers. (A) Spectra of the nanofibers after the SPAAC reaction with CH_3O-PEG-N_3 shows resonance from PEG. (B) Spectra of the nanofibers after the SPAAC reaction with CH_3O-PEG-N_3 and subsequent oxime ligation with aminooxyl-containing molecule show proton resonances from both molecules. (C) Spectra of the nanofibers after the SPAAC reaction with CH_3O-PEG-N_3, oxime ligation with aminooxyl-containing molecule. and the CuAAC reaction with 9-methyleneazidoanthracene show proton resonances from all three molecules.

N_3-GRGDS was attached to the surface of nanofibers using copper-free click chemistry by dipping the nanofibers in a N_3-GRGDS aqueous solution (1 mg/mL in water) for 5 min. The presence of GRGDS on the surface of the nanofibers was demonstrated using a GRGDS integrin mimic imaging method developed by our group.[36,57] As shown in Figure 5(A, B), GRGDS-functionalized nanofibers were highly fluorescent, while negligible fluorescence was observed in the control sample (non-N_3-GRGDS treated fibers), proving the tethered GRGDS peptide on the nanofiber surface remained bioavailable for interacting with the integrin mimic. The content of GRGDS on the nanofibers was calculated using the Lowry assay, to be 13.1 ± 5.2 μg/mg. NH_2O-dopamine was synthesized as described in the Supporting Information. NH_2O-dopamine was conjugated to the nanofibers by immersing the GRGDS-functionalized nanofibers in an aqueous solution (1 mg/mL, pH = 4.5 1 mM NaAc/AcOH buffer) of NH_2O-dopamine for 5 min. The presence of dopamine was confirmed by UV−visible spectroscopy. As shown in Figure 5C, we observed a slight absorbance decrease in the $\pi-\pi^*$ transition at 306 nm and a slight absorbance increase in the 280−286 nm region. The absorbance change at 306 nm was due to the triazole formation in the copper-free click reaction, while the intensity increase at 280−286 nm was due to conjugation of dopamine to the surface of the nanofiber mat. The dopamine concentration was further calculated to be 16.0 ± 3.2 μg/mg using a calibration curve of NH_2O-dopamine in solution. To demonstrate the successful conjugation of BMP-2 by CuAAC, the GRGDS-N_3 and NH_2O-dopamine-modified nanofibers were further treated with N_3-BMP-2-biotin. The presence of BMP-2-biotin on the nanofiber surface was proven using a complementary streptavidin-rhodamine fluorescent probe. Figure 5(D, F) shows the red fluorescence present as a result of the BMP-2-biotin-modified nanofibers, while the control nanofibers

DOI: 10.1021/mz500759n
ACS Macro Lett. 2015, 4, 207−213

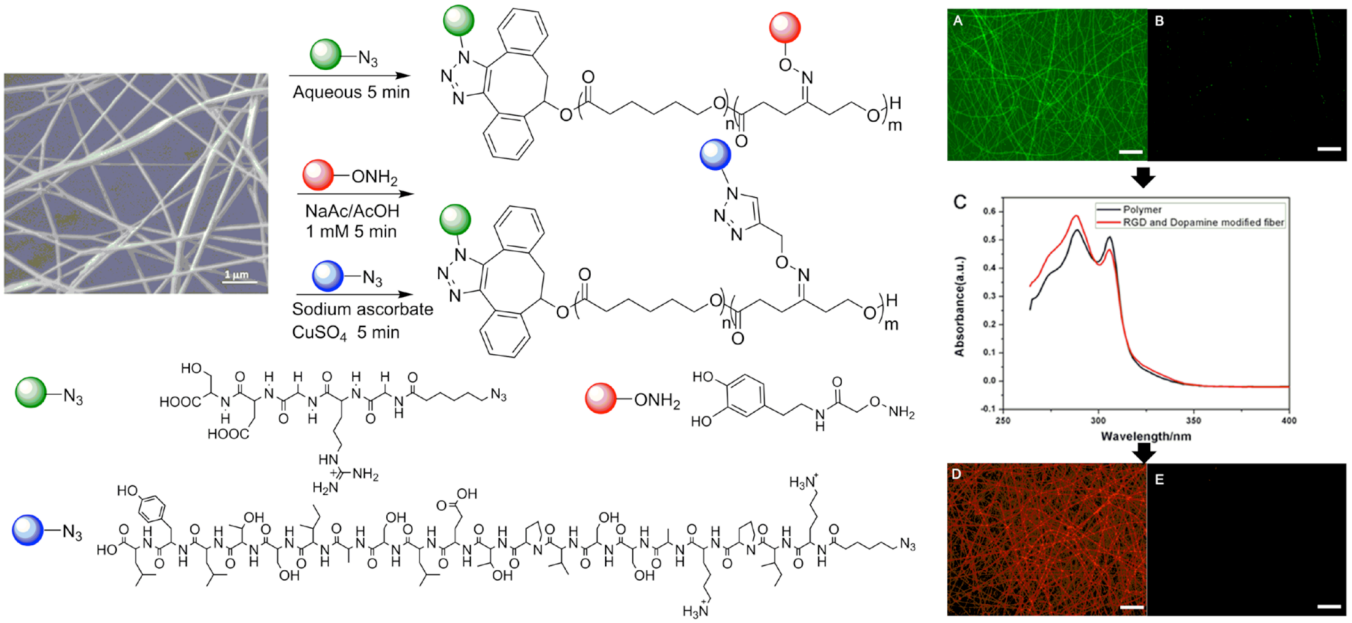

Figure 5. Fluorescence image of GRGDS modified nanofibers (A); a control experiment showing no fluorescence for non-GRGDS-treated nanofibers (B); UV−visible absorbance spectra of dopamine-functionalized nanofibers demonstrating about 16% of the available ketone groups reacted with NH_2O-dopamine by comparing the 288 nm peak to a NH_2O-dopamine solution of known concentration (C). A fluorescence image of BMP-2 peptide functionalized nanofibers (D) and a control experiment showing no fluorescence confirm the orthogonal nature of the reaction (E). The scale bar is 50 μm for all fluorescence images.

(reacted with GRGDS and dopamine) treated with N_3-BMP-2-biotin without the necessary Cu catalyst showed no fluorescence. In this case, the loading of N_3-BMP-2-biotin was specifically induced by the CuAAC reaction. Collectively these data prove the surface availability of each of the functional groups and particularly that the DIBO groups on the surface react efficiently with GRGDS-N_3 in the strained alkyne cycloaddition reaction in the first step. Assuming approximately 20% of the DIBO groups are present on the surface, only a very small quantity of GRGDS peptide (0.006 mg) is needed for 1 mg of nanofibers, which suggests that the method is translationally relevant. In a translational application, BMP-2 rather than BMP-2-biotin would be utilized. Separately, to quantify the concentration of BMP-2 on the nanofibers, N_3-BMP-2 was used instead of N_3-BMP-2-biotin following consumption of the strained cyclooctyne using azide-labeled oligoethylene glycol. The concentration of BMP-2 peptide on the surface of the nanofibers was calculated using the Lowry assay to be 13.2 ± 5.1 μg/mg. Biological experiments highlighting the concentration optimization and the collective influence of these molecules on human mesenchymal stem cell differentiation and osteoblastic mineralization *in vitro* and *in vivo* are ongoing.

In summary, we have demonstrated a sequentially triclickable nanofiber-based scaffold using DIBO-initiated ring-opening copolymerization and electrospinning. The combination of SPAAC, oxime reaction, and CuAAC yielded a robust methodology for sequential trifunctionalization of biodegradable nanofiber scaffolds. We further demonstrated the application of this methodology to tether multiple bioactive molecules to the scaffold with envisioned applications in the study of synergistic effects on cellular activity regulation. The sequential and well-controlled loading enables the conjugation of each molecule separately and quantitatively, which is highly significant for mimicking the complicated and flexible native extracellular matrix environment.

■ ASSOCIATED CONTENT

Supporting Information

The synthesis and characterization details of all compounds are provided. This material is available free of charge via the Internet at http://pubs.acs.org.

■ AUTHOR INFORMATION

Corresponding Author

*Phone: (330) 972-2834. E-mail: becker@uakron.edu.

Notes

The authors declare no competing financial interest.

■ ACKNOWLEDGMENTS

The authors are grateful for financial support from the National Science Foundation (DMR-BMAT-1105329). Mass spectrometry was provided by Kai Guo and Professor Chrys Wesdemiotis using equipment purchased with funds from the National Science Foundation (CHE-1012636 and DMR-0821313).

■ REFERENCES

(1) Ma, Z.; Kotaki, M.; Inai, R.; Ramakrishna, S. *Tissue Eng.* **2005**, *11*, 101−109.
(2) Reneker, D. H.; Yarin, A. L. *Polymer* **2008**, *49* (10), 2387−2425.
(3) Lim, S. H.; Liu, X. Y.; Song, H.; Yarema, K. J.; Mao, H.-Q. *Biomaterials* **2010**, *31* (34), 9031−9039.
(4) Subramony, S. D.; Dargis, B. R.; Castillo, M.; Azeloglu, E. U.; Tracey, M. S.; Su, A.; Lu, H. H. *Biomaterials* **2013**, *34* (8), 1942−1953.
(5) Kim, T. G.; Park, T. G. *Tissue Eng.* **2006**, *12* (2), 221−233.
(6) Yoo, H. S.; Kim, T. G.; Park, T. G. *Adv. Drug Delivery Rev.* **2009**, *61*, 1033−1042.

DOI: 10.1021/mz500759n
ACS Macro Lett. 2015, 4, 207−213

(7) Mattanavee, W.; Suwantong, O.; Puthong, S.; Bunaprasert, T.; Hoven, V. P.; Supaphol, P. *ACS Appl. Mater. Interfaces* **2009**, *1* (5), 1076−1085.
(8) Tischer, T.; Rodriguez-Emmenegger, C.; Trouillet, V.; Welle, A.; Schueler, V.; Mueller, J. O.; Goldmann, A. S.; Brynda, E.; Barner-Kowollik, C. *Adv. Mater.* **2014**, *26* (24), 4087−4092.
(9) Yu, J.; Lee, A.-R.; Lin, W.-H.; Lin, C.-W.; Wu, Y.-K.; Tsai, W.-B. *Tissue. Eng., Part A* **2014**, *20* (13−14), 1896−1907.
(10) Yang, Q.; Wu, J.; Li, J.-J.; Hu, M.-X.; Xu, Z.-K. *Macromol. Rapid Commun.* **2006**, *27* (22), 1942−1948.
(11) Jang, J.-H.; Castano, O.; Kim, H.-W. *Adv. Drug Delivery Rev.* **2009**, *61* (12), 1065−1083.
(12) Shaw, D.; Shoichet, M. *J. Craniofacial Surg.* **2003**, *14* (3), 308−316.
(13) Cho, Y. I.; Choi, J. S.; Jeong, S. Y.; Yoo, H. S. *Acta Biomater.* **2010**, *6* (12), 4725−4733.
(14) Low, W. C.; Rujitanaroj, P.-O.; Lee, D.-K.; Messersmith, P. B.; Stanton, L. W.; Goh, E.; Chew, S. Y. *Biomaterials* **2013**, *34* (14), 3581−3590.
(15) Ma, Z.; Kotaki, M.; Yong, T.; He, W.; Ramakrishna, S. *Biomaterials* **2005**, *26* (15), 2527−2536.
(16) Ma, Z.; He, W.; Yong, T.; Ramakrishna, S. *Tissue. Eng.* **2005**, *11* (7−8), 1149−1158.
(17) Cowan, C. M.; Jiang, X.; Hsu, T.; Soo, C.; Zhang, B.; Wang, J. Z.; Kuroda, S. i.; Wu, B.; Zhang, Z.; Zhang, X.; Ting, K. *J. Bone Miner. Res.* **2007**, *22* (6), 918−930.
(18) Smith Callahan, L. A.; Xie, S.; Barker, I. A.; Zheng, J.; Reneker, D. H.; Dove, A. P.; Becker, M. L. *Biomaterials* **2013**, *34* (36), 9089−9095.
(19) Yang, L.; Anderson, D. E.; Baecher-Allan, C.; Hastings, W. D.; Bettelli, E.; Oukka, M.; Kuchroo, V. K.; Hafler, D. A. *Nature* **2008**, *454* (7202), 350−352.
(20) Tang, W.; Becker, M. L. *Chem. Soc. Rev.* **2014**, *43*, 7013−7039.
(21) Mahmoud, Z. N.; Gunnoo, S. B.; Thomson, A. R.; Fletcher, J. M.; Woolfson, D. N. *Biomaterials* **2011**, *32* (15), 3712−3720.
(22) Lancuški, A.; Bossard, F.; Fort, S. *Biomacromolecules* **2013**, *14* (6), 1877−1884.
(23) Goldmann, A. S.; Tischer, T.; Barner, L.; Bruns, M.; Barner-Kowollik, C. *Biomacromolecules* **2011**, *12* (4), 1137−1145.
(24) Tischer, T.; Goldmann, A. S.; Linkert, K.; Trouillet, V.; Börner, H. G.; Barner-Kowollik, C. *Adv. Funct. Mater.* **2012**, *22* (18), 3853−3864.
(25) Zhu, Y.; Mao, Z.; Gao, C. *RSC Adv.* **2013**, *3* (8), 2509−2519.
(26) Lutz, J. F. *Angew. Chem., Int. Ed.* **2008**, *47*, 2182−2184.
(27) Sletten, E. M.; Bertozzi, C. R. *Angew. Chem., Int. Ed.* **2009**, *48* (38), 6974−6998.
(28) Mbua, N. E.; Guo, J.; Wolfert, M. A.; Steet, R.; Boons, G.-J. *ChemBioChem* **2011**, *12* (12), 1912−1921.
(29) Beatty, K. E.; Fisk, J. D.; Smart, B. P.; Lu, Y. Y.; Szychowski, J.; Hangauer, M. J.; Baskin, J. M.; Bertozzi, C. R.; Tirrell, D. A. *ChemBioChem* **2010**, *11* (15), 2092−2095.
(30) Jang, S.; Sachin, K.; Lee, H.-j.; Kim, D. W.; Lee, H. S. *Bioconjugate Chem.* **2012**, *23* (11), 2256−2261.
(31) Friscourt, F.; Ledin, P. A.; Mbua, N. E.; Flanagan-Steet, H. R.; Wolfert, M. A.; Steet, R.; Boons, G.-J. *J. Am. Chem. Soc.* **2012**, *134* (11), 5381−5389.
(32) DeForest, C. A.; Anseth, K. S. *Nat. Chem.* **2011**, *3* (12), 925−931.
(33) DeForest, C. A.; Anseth, K. S. *Angew. Chem., Int. Ed.* **2012**, *51* (8), 1816−1819.
(34) Zheng, J.; Smith Callahan, L. A.; Hao, J.; Guo, K.; Wesdemiotis, C.; Weiss, R. A.; Becker, M. L. *ACS Macro Lett.* **2012**, *1* (8), 1071−1073.
(35) Azagarsamy, M. A.; Anseth, K. S. *ACS Macro Lett.* **2012**, *2* (1), 5−9.
(36) Zheng, J.; Liu, K.; Reneker, D. H.; Becker, M. L. *J. Am. Chem. Soc.* **2012**, *134* (41), 17274−17277.
(37) Zheng, J.; Xie, S.; Lin, F.; Hua, G.; Yu, T.; Reneker, D. H.; Becker, M. L. *Polym. Chem.* **2013**, *4* (7), 2215−2218.
(38) Lin, F.; Zheng, J.; Yu, J.; Zhou, J.; Becker, M. L. *Biomacromolecules* **2013**, *14* (8), 2857−2865.
(39) Orski, S. V.; Poloukhtine, A. A.; Arumugam, S.; Mao, L.; Popik, V. V.; Locklin, J. *J. Am. Chem. Soc.* **2010**, *132* (32), 11024−11026.
(40) Ma, Y.; Zheng, J.; Amond, E. F.; Stafford, C. M.; Becker, M. L. *Biomacromolecules* **2013**, *14* (3), 665−671.
(41) Singh, I.; Wendeln, C.; Clark, A. W.; Cooper, J. M.; Ravoo, B. J.; Burley, G. A. *J. Am. Chem. Soc.* **2013**, *135* (9), 3449−3457.
(42) Su, H.; Zheng, J.; Wang, Z.; Lin, F.; Feng, X.; Dong, X.-H.; Becker, M. L.; Cheng, S. Z. D.; Zhang, W.-B.; Li, Y. *ACS Macro Lett.* **2013**, *2* (8), 645−650.
(43) Grover, G. N.; Lee, J.; Matsumoto, N. M.; Maynard, H. D. *Macromolecules* **2012**, *45* (12), 4958−4965.
(44) Flavell, R. R.; Kothari, P.; Bar-Dagan, M.; Synan, M.; Vallabhajosula, S.; Friedman, J. M.; Muir, T. W.; Ceccarini, G. *J. Am. Chem. Soc.* **2008**, *130* (28), 9106−9112.
(45) Rusmini, F.; Zhong, Z.; Feijen, J. *Biomacromolecules* **2007**, *8* (6), 1775−1789.
(46) Christman, K. L.; Schopf, E.; Broyer, R. M.; Li, R. C.; Chen, Y.; Maynard, H. D. *J. Am. Chem. Soc.* **2008**, *131* (2), 521−527.
(47) Lin, F.; Yu, J.; Tang, W.; Zheng, J.; Defante, A.; Guo, K.; Wesdemiotis, C.; Becker, M. L. *Biomacromolecules* **2013**, *14*, 3749−3758.
(48) Grover, G. N.; Lam, J.; Nguyen, T. H.; Segura, T.; Maynard, H. D. *Biomacromolecules* **2012**, *13* (10), 3013−3017.
(49) Tian, D.; Dubois, P.; Grandfils, C.; Jérôme, R. *Macromolecules* **1997**, *30* (3), 406−409.
(50) Acharya, A. P.; Dolgova, N. V.; Moore, N. M.; Xia, C.-Q.; Clare-Salzler, M. J.; Becker, M. L.; Gallant, N. D.; Keselowsky, B. G. *Biomaterials* **2010**, *31* (29), 7444−7454.
(51) Smith Callahan, L. A.; Policastro, G. M.; Bernard, S. L.; Childers, E. P.; Boettcher, R.; Becker, M. L. *Biomacromolecules* **2013**, *14* (9), 3047−3054.
(52) Salinas, C. N.; Anseth, K. S. *J. Tissue Eng. Regener. Med.* **2008**, *2* (5), 296−304.
(53) Ryu, J.; Ku, S. H.; Lee, H.; Park, C. B. *Adv. Funct. Mater.* **2010**, *20* (13), 2132−2139.
(54) Cao, L.; Wang, J.; Hou, J.; Xing, W.; Liu, C. *Biomaterials* **2014**, *35* (2), 684−698.
(55) Lee, S. S.; Huang, B. J.; Kaltz, S. R.; Sur, S.; Newcomb, C. J.; Stock, S. R.; Shah, R. N.; Stupp, S. I. *Biomaterials* **2013**, *34* (2), 452−459.
(56) Moore, N. M.; Lin, N. J.; Gallant, N. D.; Becker, M. L. *Acta Biomater.* **2011**, *7* (5), 2091−2100.
(57) Morgan, A. W.; Roskov, K. E.; Lin-Gibson, S.; Kaplan, D. L.; Becker, M. L.; Simon, C. G., Jr. *Biomaterials* **2008**, *29* (16), 2556−2563.

DOI: 10.1021/mz500759n
ACS Macro Lett. 2015, 4, 207−213